Anisotropic backscatter in ice-penetrating radar data - potential mechanisms and implications

R. Drews[1,2], O. Eisen[1], W. Rack[2], D. Steinhage[1], I. Weikusat[1]

[1]: Alfred Wegener Institute for Polar and Marine Research, Bremerhaven, Germany [2]: Gateway Antarctica, University of Canterbury, Christchurch, New Zealand

D. Steinhage

Introduction

Ice-penetrating what ?

Ice-penetrating radar measures internal stucture and thickness of glaciers and ice sheets, by recording the two-way travel time of reflections from previously emitted (electromagnetic) pulses. Internal reflections are mainly caused by non-uniformities in density, conductivity and crystal orientation fabric (COF) (Fujita1999) which alter the dielectric properties. In order to pinpoint the reflection mechanisms multi-frequency and multi-polarization surveys are needed.

What is anisotropic backscatter ?

The reflection mechanism is anisotropic (or direction dependent), if the reflected power is dependent on the incoming polarization. The term 'backscattered' is used instead of 'reflected' when the signal originates from a conglomerate of distributed targets.


(1a)　**(1b)**
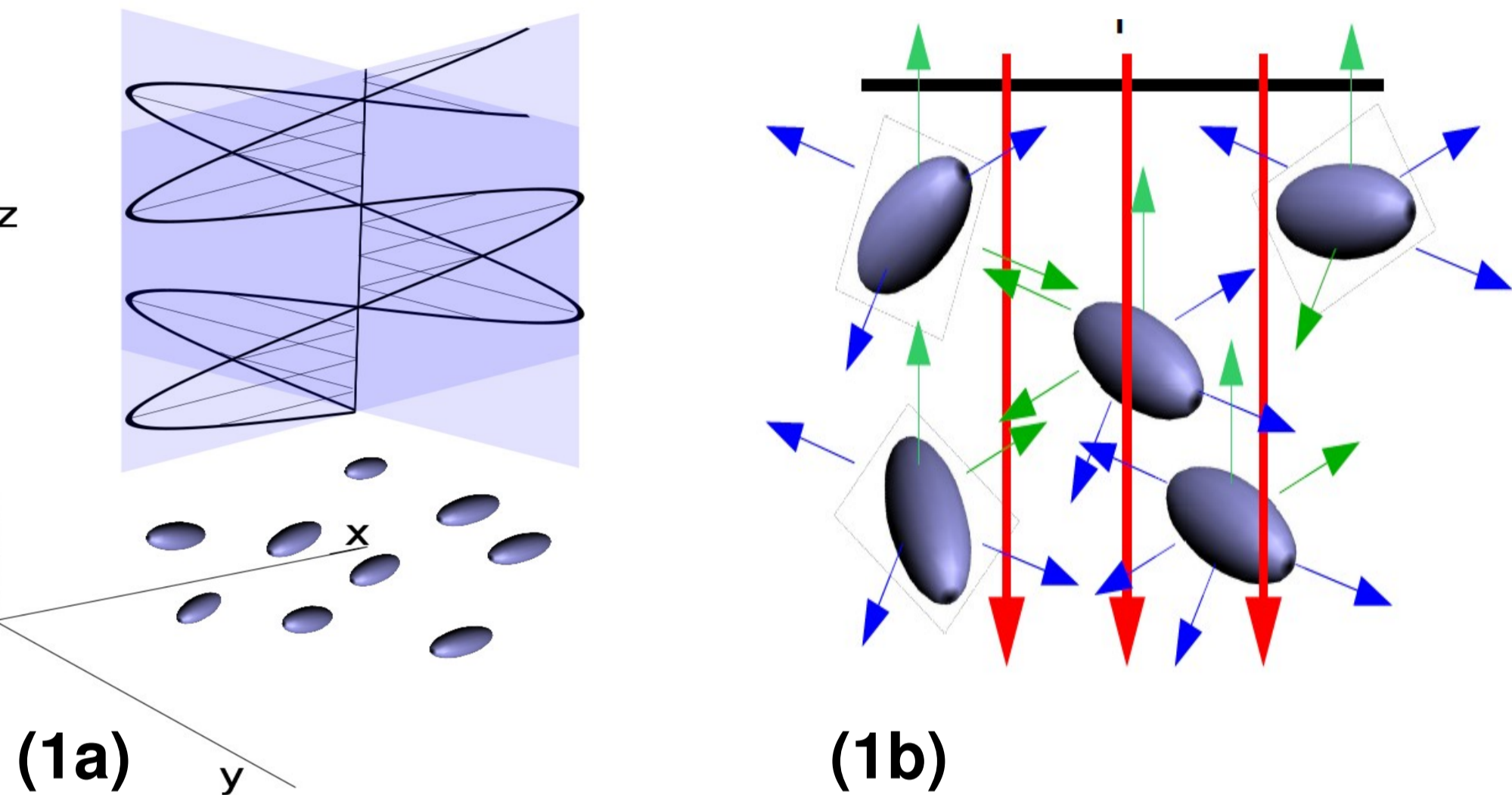
What is new about this study?

Due to the layer-like architecture of icesheets, most internal reflections are mathematically treated as surface reflections. In this study we don't focus on individual layers (as done by Eisen2007), but on the bulk properties, which alter the background level of the acquired signal. We develop analytical volume scattering models to quantify the effect of anisotropic airbubbles and varying COF along the ice-column.
Anisotropic airbubbles or preferred COF may serve as strain markers in the ice. Mapped via remote sensing, it serves as input for ice-sheet modelling.

Observation

In a sample dataset at Kohnen (Antarctica) we see a strong polarization dependence in the upper third of the ice column.
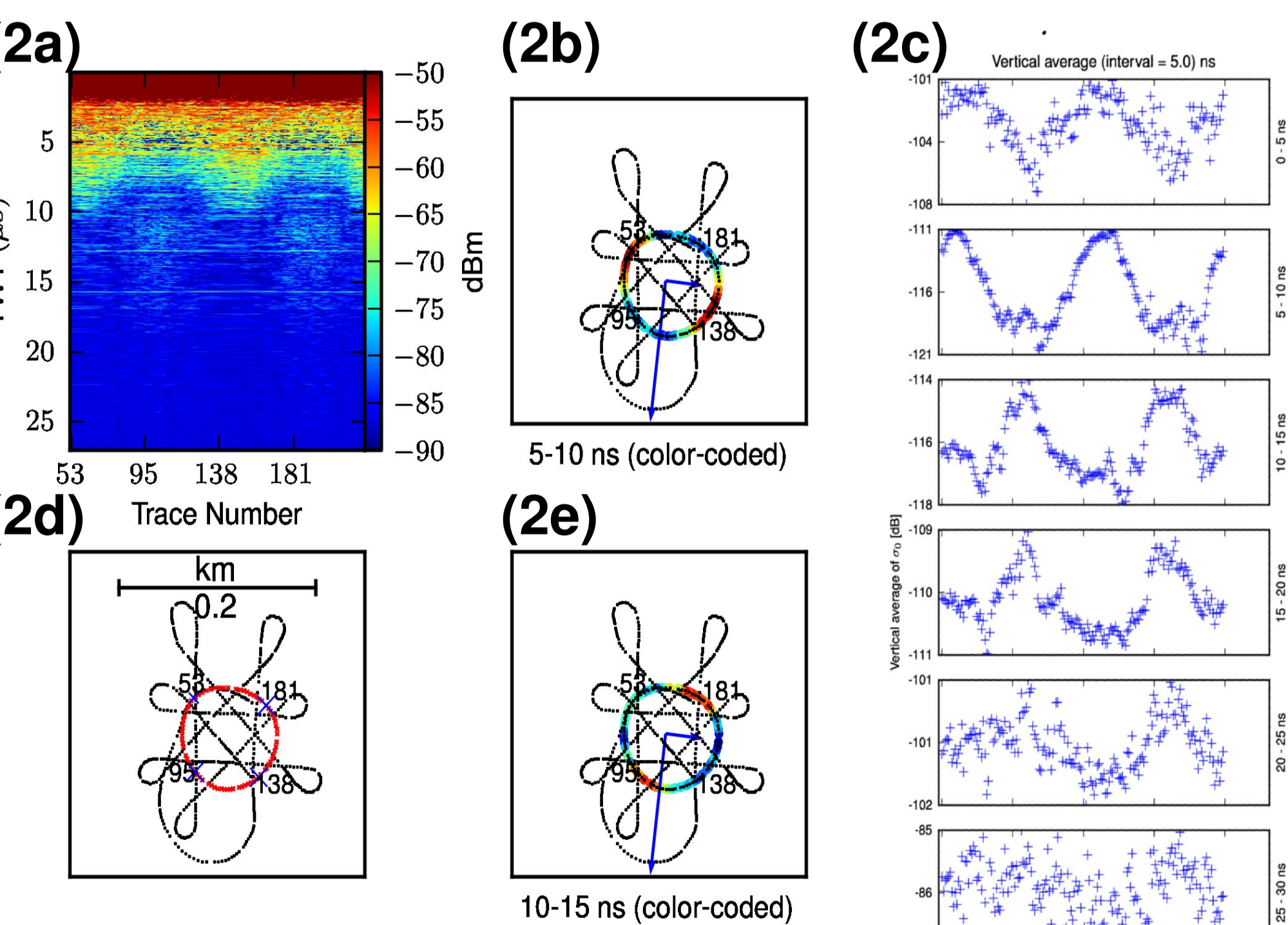
Circular radar profile (airplane on the ground)
(2a): Backscattered power of circular radar profile shown in **(2c)**; **(2b),(2e):** The sinusoidal pattern exhibits a 180°- symmetry. In the upper 400 – 900 m (~5–10μs TWT) it is maximal in the direction of minimal surface strain. From 900 m down to ~1300 m (~15μs TWT) the pattern shifts by 90°; **(2c)** the depth averaged attenuation corrected profile shows changes in reflection power of ~3–5 dB. A 45° symmetry pointing to birefringence is not dominating.

Method

Analytical Model with Radiative Transfer Theory:

For quantifying the effect of anisotropic inclusions, we adapt a model previously used for satellite remote sensing applications of canopy (Tsang1981).

$$\cos(\theta)\frac{d\mathbf{I}}{dz} = -\underline{\mathbf{k_e}}\mathbf{I}(\theta,\phi,z) + \int_0^{2\pi} d\phi' \int_0^{\pi/2} d\theta' \sin(\theta') \underline{\mathbf{P}}(\theta,\phi,\theta',\phi') \cdot \mathbf{I}$$

θ : incoming angle
$\mathbf{I}$: mod. Stokes Vector of incoming Intensity
$\mathbf{k_e} := \mathbf{k_s} + \mathbf{k_a}$ Extinction Matrix
$\mathbf{P}(\theta,\phi,\theta',\phi')$: Phasematrix (Scattering from:(θ,ϕ)nach(θ',ϕ'))

Free parameters (with Phasematrix elements):

· Orientation distribution via Euler angles
· Volume fraction
· Bubble volume
· Eccentricity
· Angular dependcy of incoming radiation

Iterative solution:

0th order: extinction only
1th order: independent (Rayleigh) scattering
2th order: first order multiple scattering

(3a)　**(3b)**　**(3c)**

Graphic modified from Lionel Brits
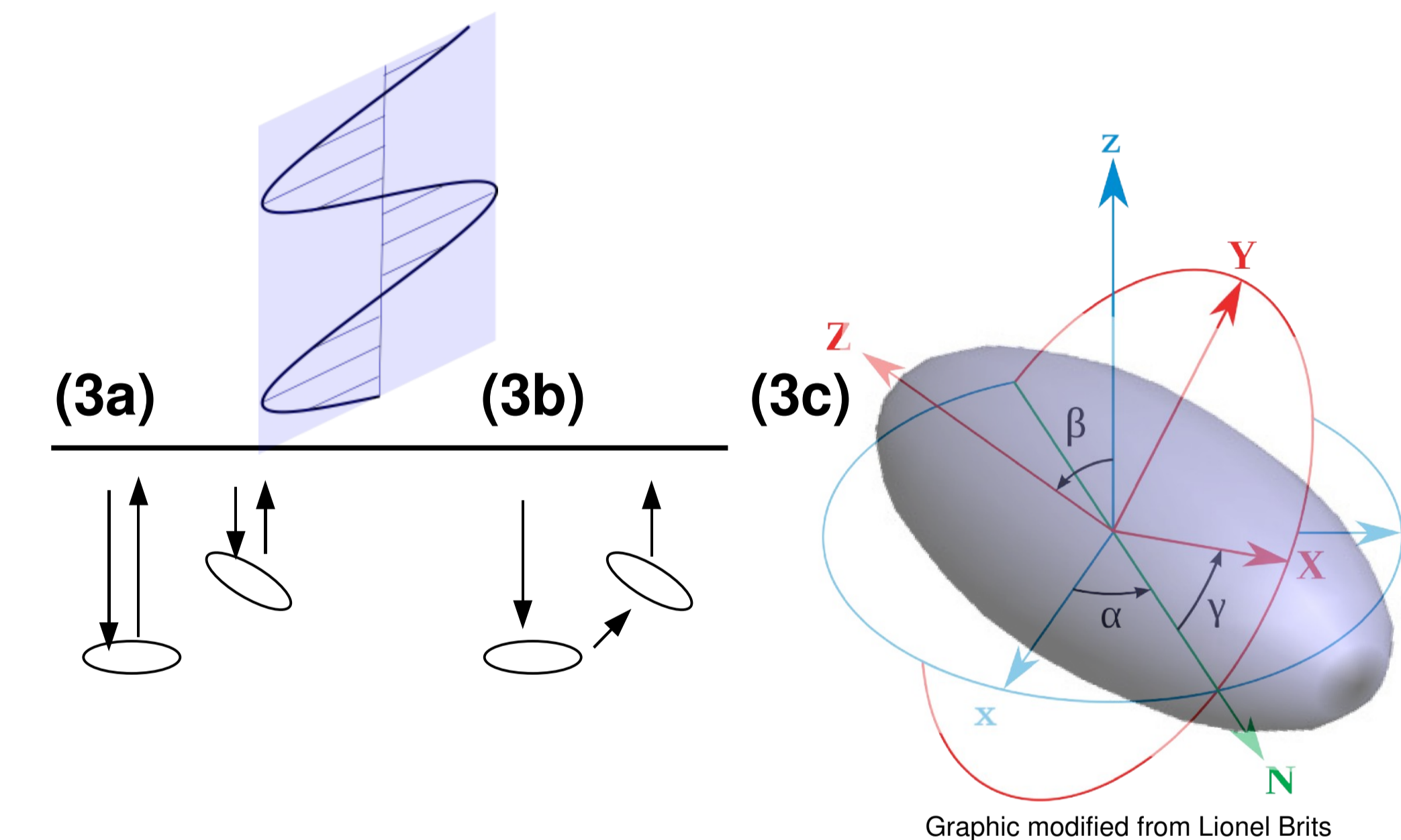
Graphical representation of model setup
(3a): The first order iteration includes independent rayleigh scattering only, **(3b)** illustrates one out of many second order contributions. **(3c)** Visualizes the Euler angles, which are used to define the orientation distribution of the air bubbles.

Model test and outcomes:

➡ Treat horizontal and vertical polarization in a limit for vertical incidence

(4a)　**(4b)**
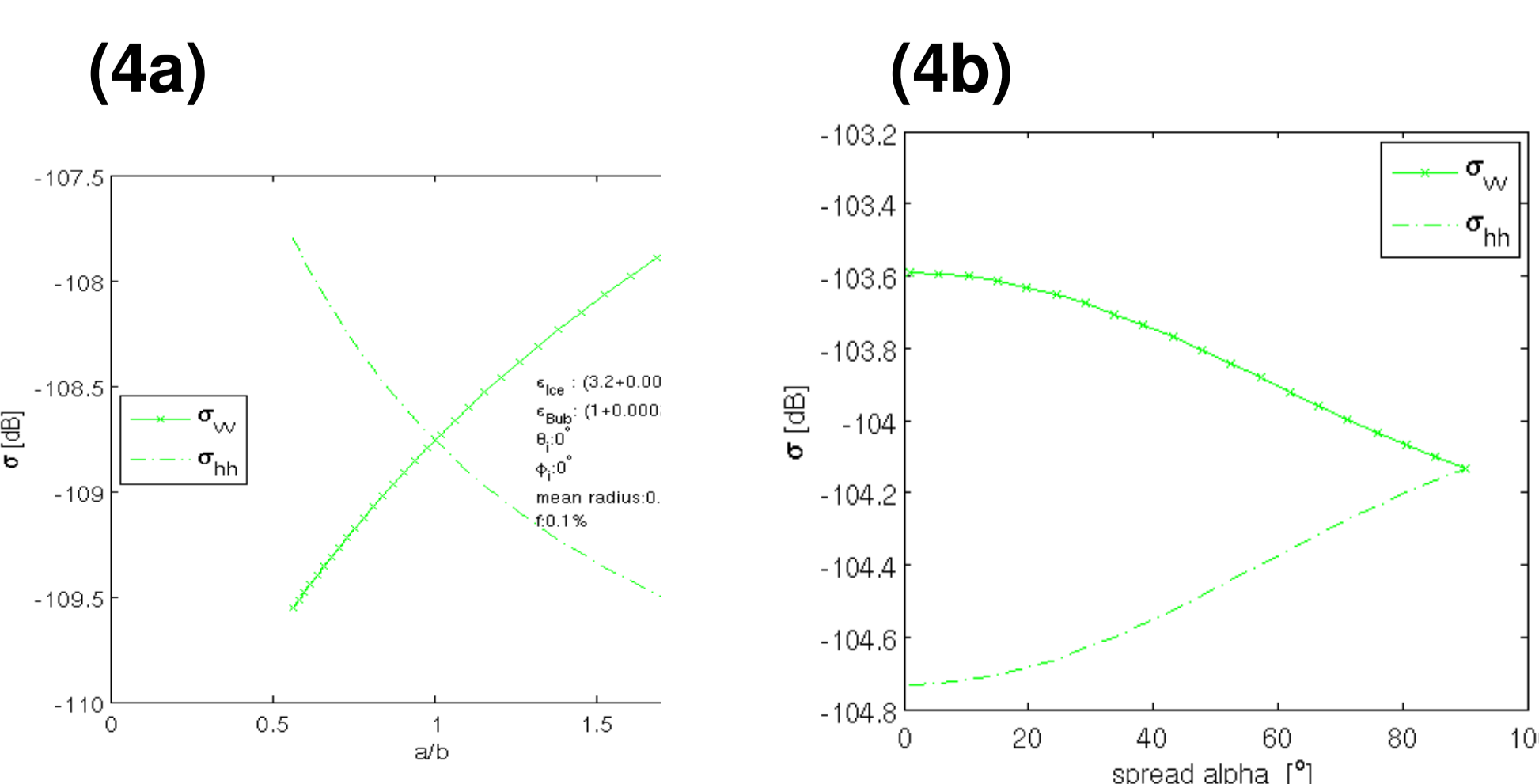
Test w.r.t symmetries
(4a): Interchanging the horizontal semi-axis (a,b) while keeping the bubble volume constant. As expected for a/b=1 there is no polarization dependence (but depolarisation due to multiple scattering (not shown); **(4a):** Simulating the transition from a fully aligned bubble distribution (in the horizontal) to an entire random distribution. As expected no polarization dependence for the fully random case.


(5a)　**(5b)**

(5a)　**(5b)**
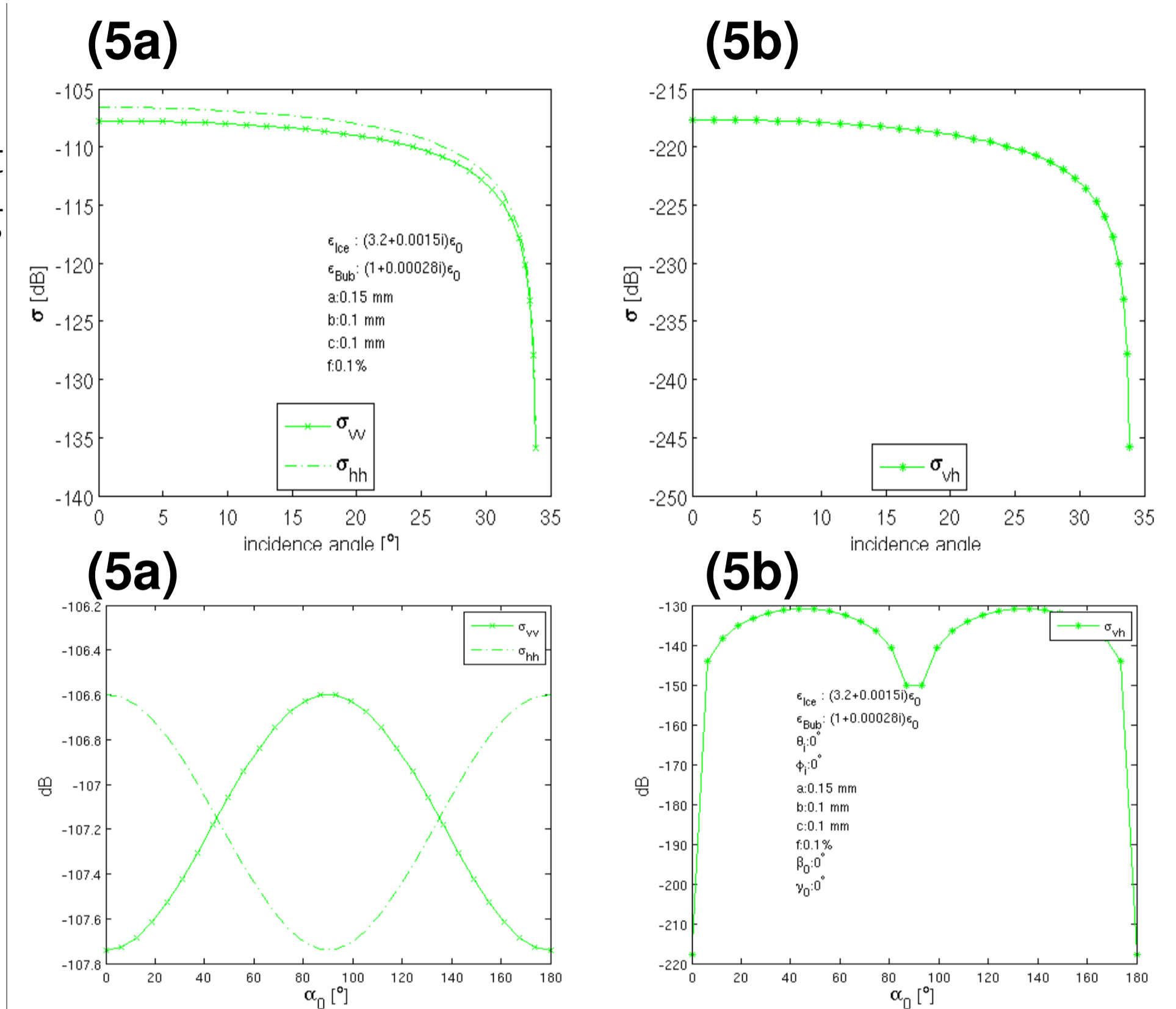
(5a): Run for a varying incidence angle. Bubbles are oriented in the horizontal plane. **(5a):** Run for nadir incidence, with bubbles rotating in the horizontal plane. This mimics the circular profile shown in (2a). The symmetries are reproduced, but the effect is small.

Conclusions

- **Analytical model improves understanding of the (volume) scattering process**
- **Expected symmetries can be reproduced**
- **Depolarisation occurs as a first or second order effect (depending on the configuration)**
- **Effect of enclosed air bubbles probably too small**

Similar Model for COF scattering is needed!

Outlook
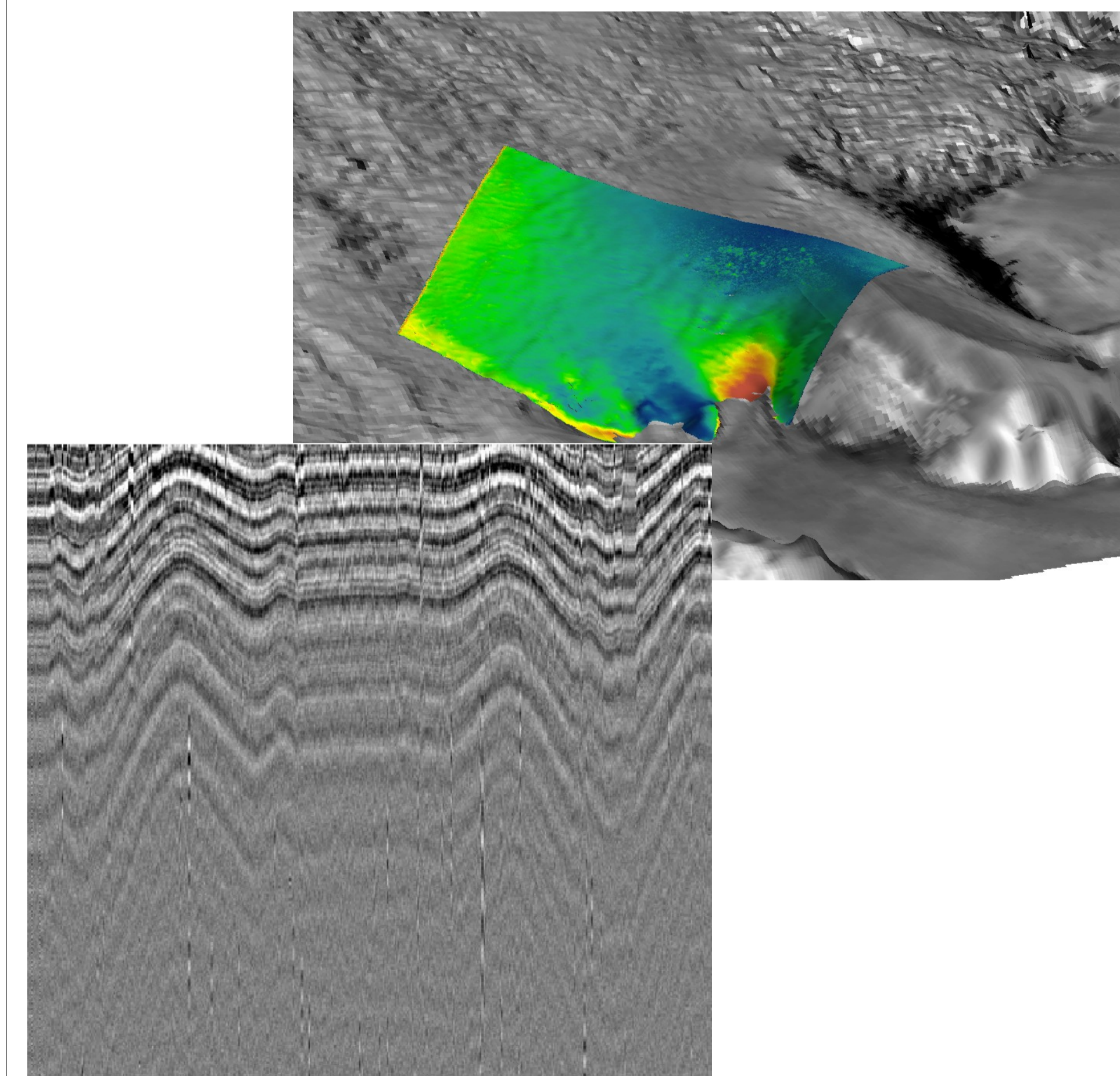
A combined approach of InSAR (see N. Neckel's poster) and polarimetric GPR surveys help to characterise complex flow regimes (e. g. around triple points). Important implications for age-depth modelling and flow dynamics in general.

Fujita et al., *Radio-wave depolarization and scattering within ice sheets: a matrix-based model to link radar and ice-core measurements and its application*, J. Glaciol., 52(178), 407–424, 2006.
Eisen et al., *Direct evidence for continuous radar reflector originating from changes in crystal-orientation fabric*, The Cryosphere, 1, 1–10, 2007
Tsang et al., *Radiative transfer theory for active remote sensing of a layer of small ellipsoidal scatterers*, Radio Science, Volume 46, No. 3, 1981